# SI Appendix

## Materials and Methods

### Protein Expression and Purification Details

#### p-Nephrin

p-Nephrin was made similarly to what was previously described (1, 2). Nephrin was tagged with Maltose binding protein (MBP) at the N-terminus to enhance solubility and expression. This protein was expressed in BL21(DE3)T1R cells at 30 °C through induction with 1 mM IPTG for 7 hours. Cells were harvested in buffer (20 mM Tris pH 8, 20 mM imidazole, 150 mM NaCl, 5 mM βME, 0.01% NP-40, 10 % glycerol, 1 mM PMSF, 1 µg/mL Antipain, 1 mM Benzamidine and 1 µg/mL Leupeptin), lysed using a homogenizer (Emulsiflex-C5, Avestin), and collected by centrifugation. Cleared lysate was then applied to Ni-NTA agarose (Qiagen), washed with the lysis buffer containing 300 mM NaCl and 50 mM imidazole, and eluted with the same buffer but containing 150 mM NaCl and 300 mM imidazole. The MBP was removed with TEV protease treatment, and simultaneously the $His_6$-tag was removed with PreScission protease treatment at 4 °C for 16 hours or at room temperature for 2 hours. The protein was further purified using a Source 15Q column (GE Healthcare), applied through a gradient of 150 300 mM NaCl in 20 mM Imidazole pH 8, 1 mM EDTA and 2 mM DTT, followed by an SD200 column (GE Healthcare) run in 25 mM Hepes pH 7.5, 150 mM NaCl, 1 mM $MgCl_2$ , and 2 mM βME. Fractions containing Nephrin were concentrated using an Amicon Ultra 3 K concentrator.

Nephrin was then phosphorylated at 30 °C with 20 nM Lck kinase overnight or with 500 nM Lck for 1 hour. The phosphorylation reaction was quenched with 10 mM EDTA. Kinase and incompletely phosphorylated Nephrin were removed using a source 15 Q column evolved with a gradient of 150 250 mM NaCl in 25 mM Hepes pH 7 and 2 mM βME. The phosphorylated product was further purified using an SD200 column (GE Healthcare) in 150KMEI buffer (150 mM KCl, 1 mM $MgCl_2$, 1 mM EGTA, 10 mM Imidazole pH 7.0 and 1 mM DTT). Complete phosphorylation was ascertained using mass spectrometry.

**Nck**

GST-Nck was expressed and purified identically as previously described (1)) through a GST column, a Source 15 Q column, a Source 15 S column and a SD200 column. The protein was flash-frozen in 150KMEI buffer (150 mM KCl, 1 mM $MgCl_2$, 1 mM EGTA, 10 mM Imidazole pH 7.0 and 1 mM DTT).

Mutants and fragments of Nck were purified similarly to the full-length wild type protein. A summary of the purification steps for these proteins is provided in Table S2.

**N-WASP**

$His_6$-N-WASP (BPVCA construct) was expressed and purified as described (1) through Ni-NTA, Source 15Q, TEV cleavage, Source 15S and SD200. Finally, the protein was flash-frozen in 150KMEI buffer (150 mM KCl, 1 mM $MgCl_2$, 1 mM EGTA, 10 mM Imidazole pH 7.0 and 1 mM DTT).

**Lck, Actin and Arp2/3**

$His_6$-Lck kinase was expressed from baculovirus in *Spodoptera frugiperta* (Sf9) cells and purified as described previously (1). Actin and Arp2/3 complex were purified as described previously (3).

For isotopic labeling, cultures were grown in M9 minimal media containing $^{15}NH_4Cl$ or $^{13}C$ glucose (Cambridge Isotopes) as the sole nitrogen and carbon sources and induced at an OD of 0.8 with 1 mM IPTG. The proteins were harvested and purified similarly to full length Nck, and as summarized in Table S2.

**SUMO-SIM Proteins**

$SUMO_5$-$SIM_5$ and $SUMO_5$-L1-$SIM_5$ were expressed in BL21(DE3)T1R cells at 18 °C through overnight induction with 1 mM IPTG. Cells were collected by centrifugation and lysed by homogenization in (20 mM Tris pH 8, 1 mM PMSF, 1 µg/mL Antipain, 1 mM Benzamidine, 1 µg/mL Leupeptin and 1 µg/mL Pepstatin). The cleared lysate was applied to Ni-NTA agarose beads (Qiagen), washed with 5 column volumes of 50 mM NaCl, 50 mM Tris pH 8, 20mM Imidazole, and eluted

with 5 column volumes of 50 mM NaCl, 50 mM tis pH 8, 300 mM Imidazole. Elution was then applied to Amylose Resin (NEB), washed in 5 column volumes 50 mM tris pH 8, 50 mM NaCl, 1 mM EDTA, and eluted in 5 column volumes 50 mM tris pH 8, 50 mM NaCl, 1 mM EDTA, 50 mM maltose. The MBP and polyhistidine tags were removed with TEV protease treatment at room temperature for 3-4 hours. Cleaved $SUMO_5$-$SIM_5$ or $SUMO_5$-L1-$SIM_5$ was applied to a Source 15Q column using a gradient of 100 → 500 mM NaCl in 20 mM tris pH 8, 1 mM EDTA. Fractions containing fusion proteins were pooled and applied to an SD200 column (GE). Pooled fractions were concentrated using an Amicon Ultra 10k concentrator (Millipore), and flash-frozen in 10 mM tris pH 8 and 50 mM NaCl.

**Table S1. Sequences of the proteins/peptidesPRM used in this study**

| Construct | Sequence | Notes |
|---|---|---|
| N-WASP (BPVCA) | GHMGSEFKEKKKGKAKKKRAPPPPPPSRGGPPPPPPPPHSSGPPPPPARGRGAPPPPPSRAPTAAPPPPPPSRPGVVVPPPPPPNRMYPHPPPALPSSAPSGPPPPPPLSMAGSTAPPPPPPPPPPPGPPPPPGLPSDGDHQVPASSGNKAALLDQIREGAQLKKVEQNSRPVSCSGRDALLDQIRQGIQLKSVSDGQESTPPTPAPTSGIVGALMEVMQKRSKAIHSSDEDEDDDDEEDFEDDDEWED | Rat, residues 183-193 fused to 273-501 |
| Nephrin 3Y | GHMHLYDEVERTFPPSGAWGPLYDEVQMGPWDLHWPEDTFQDPRGIYDQVAGD | Human, residues 1174-1223, Y1183F, Y1210F |

| | | |
|---|---|---|
| Nck | GHMAEEVVVVAKFDYVAQQEQELDIKKNERLWLLDDSKSW<br>WRVRNSMNKTGFVPSNYVERKNSARKASIVKNLKDTLGIG<br>KVKRKPSVPDSASPADDSFVDPGERLYDLNMPAYVKFNYM<br>AEREDELSLIKGTKVIVMEKCSDGWWRGSYNGQVGWFPSN<br>YVTEEGDSPLGDHVGSLSEKLAAVVNNLNTGQVLHVVQAL<br>YPFSSSNDEELNFEKGDVMDVIEKPENDPEWWKCRKINGM<br>VGLVPKNYVTVMQNNPLTSGLEPSPPQCDYIRPSLTGKFA<br>GNPWYYGKVTRHQAEMALNERGHEGDFLIRDSESSPNDFS<br>VSLKAQGKNKHFKVQLKETVYCIGQRKFSTMEELVEHYKK<br>APIFTSEQGEKLYLVKHLS | Human, residues 1-377; S1-Red, S2-Green, S3-Blue,SH2-Brown |
| Lck | ANSLEPEPWFFKNLSRKDAERQLLAPGNTHGSFLIRESES<br>TAGSFSLSVRDFDQNQGEVVKHYKIRNLDNGGFYISPRIT<br>FPGLHDLVRHYTNASDGLCTKLSRPCQTQKPQKPWWEDEW<br>EVPRETLKLVERLGAGQFGEVWMGYYNGHTKVAVKSLKQG<br>SMSPDAFLAEANLMKQLQHPRLVRLYAVVTQEPIYIITEY<br>MENGSLVDFLKTPSGIKLNVNKLLDMAAQIAEGMAFIEEQ<br>NYIHRDLRAANILVSDTLSCKIADFGLARLIEDNEYTARE<br>GAKFPIKWTAPEAINYGTFTIKSDVWSFGILLTEIVTHGR<br>IPYPGMTNPEVIQNLERGYRMVRPDNCPEELYHLMMLCWK<br>ERPEDRPTFDYLRSVLDDFFTATEGQFQPQP | Human, 119–509, Y505F |
| S1-L1-S2-L3-SH2 | GHMAEEVVVVAKFDYVAQQEQELDIKKNERLWLLDDSKSW<br>WRVRNSMNKTGFVPSNYVERKNSARKASIVKNLKDTLGIG<br>KVKRKPSVPDSASPADDSFVDPGERLYDLNMPAYVKFNYM<br>AEREDELSLIKGTKVIVMEKSSDGWWRGSYNGQVGWFPSN<br>YVTEEGDSPLNNPLTSGLEPSPPQSDYIRPSLTGKFAGNP<br>WYYGKVTRHQAEMALNERGHEGDFLIRDSESSPNDFSVSL<br>KAQGKNKHFKVQLKETVYSIGQRKFSTMEELVEHYKKAPI<br>FTSEQGEKLYLVKHLS | Missing S3 domain; Residues1-170, 252-377, C139S, C266S, C340S |
| S1-L1-S3-L3-SH2 | GHMAEEVVVVAKFDYVAQQEQELDIKKNERLWLLDDSKSW<br>WRVRNSMNKTGFVPSNYVERKNSARKASIVKNLKDTLGIG<br>KVKRKPSVPDSASPADDSFVDPGERLYDLNVLHVVQALYP<br>FSSSNDEELNFEKGDVMDVIEKPENDPEWWKCRKINGMVG<br>LVPKNYVTVMQNNPLTSGLEPSPPQSDYIRPSLTGKFAGN<br>PWYYGKVTRHQAEMALNERGHEGDFLIRDSESSPNDFSVS<br>LKAQGKNKHFKVQLKETVYSIGQRKFSTMEELVEHYKKAP<br>IFTSEQGEKLYLVKHLS | Missing S2 domain; Residues 1-108, 191-377, C266S, C340S |
| S2-L2-S3-L3-SH2 | GHMDLNMPAYVKFNYMAEREDELSLIKGTKVIVMEKSSDG<br>WWRGSYNGQVGWFPSNYVTEEGDSPLGDHVGSLSEKLAAV<br>VNNLNTGQVLHVVQALYPFSSSNDEELNFEKGDVMDVIEK<br>PENDPEWWKCRKINGMVGLVPKNYVTVMQNNPLTSGLEPS<br>PPQSDYIRPSLTGKFAGNPWYYGKVTRHQAEMALNERGHE<br>GDFLIRDSESSPNDFSVSLKAQGKNKHFKVQLKETVYSIG<br>QRKFSTMEELVEHYKKAPIFTSEQGEKLYLVKHLS | di-SH3 construct lacking S1-L1; Residues 106-377, C139S, C266S, C340S |

| | | |
|---|---|---|
| L1-S2-L2-S3-L3-SH2 | GHMKNSARKASIVKNLKDTLGIGKVKRKPSVPDSASPADD SFVDPGERLYDLNMPAYVKFNYMAEREDELSLIKGTKVIV MEKSSDGWWRGSYNGQVGWFPSNYVTEEGDSPLGDHVGSL SEKLAAVVNNLNTGQVLHVVQALYPFSSSNDEELNFEKGD VMDVIEKPENDPEWWKCRKINGMVGLVPKNYVTVMQNNPL TSGLEPSPPQSDYIRPSLTGKFAGNPWYYGKVTRHQAEMA LNERGHEGDFLIRDSESSPNDFSVSLKAQGKNKHFKVQLK ETVYSIGQRKFSTMEELVEHYKKAPIFTSEQGEKLYLVKH LS | Missing S1; Residues 59-377, C139S, C266S, C340S |
| ΔL1-S2-L2-S3-L3-SH2 | GHMGIGKVKRKPSVPDSASPADDSFVDPGERLYDLNMPAY VKFNYMAEREDELSLIKGTKVIVMEKSSDGWWRGSYNGQV GWFPSNYVTEEGDSPLGDHVGSLSEKLAAVVNNLNTGQVL HVVQALYPFSSSNDEELNFEKGDVMDVIEKPENDPEWWKC RKINGMVGLVPKNYVTVMQNNPLTSGLEPSPPQSDYIRPS LTGKFAGNPWYYGKVTRHQAEMALNERGHEGDFLIRDSES SPNDFSVSLKAQGKNKHFKVQLKETVYSIGQRKFSTMEEL VEHYKKAPIFTSEQGEKLYLVKHLS | di-SH3 Construct lacking 17 N-terminal L1 residues; Residues 76-377, C139S, C266S, C340S |
| L1K/E S2-L2-S3-L3-SH2 | GHMKNSAREASIVENLEDTLGIGKVKRKPSVPDSASPADD SFVDPGERLYDLNMPAYVKFNYMAEREDELSLIKGTKVIV MEKSSDGWWRGSYNGQVGWFPSNYVTEEGDSPLGDHVGSL SEKLAAVVNNLNTGQVLHVVQALYPFSSSNDEELNFEKGD VMDVIEKPENDPEWWKCRKINGMVGLVPKNYVTVMQNNPL TSGLEPSPPQSDYIRPSLTGKFAGNPWYYGKVTRHQAEMA LNERGHEGDFLIRDSESSPNDFSVSLKAQGKNKHFKVQLK ETVYSIGQRKFSTMEELVEHYKKAPIFTSEQGEKLYLVKH LS | N-terminal charges mutated (K to E); Residues 59-377, C139S, C266S, C340S |
| L1Δ(KVKRK)-S2-L2-S3-L3-SH2 | GHMKNSARKASIVKNLKDTLGIG(GS)PSVPDSASPADDS FVDPGERLYDLNMPAYVKFNYMAEREDELSLIKGTKVIVM EKSSDGWWRGSYNGQVGWFPSNYVTEEGDSPLGDHVGSLS EKLAAVVNNLNTGQVLHVVQALYPFSSSNDEELNFEKGDV MDVIEKPENDPEWWKCRKINGMVGLVPKNYVTVMQNNPLT SGLEPSPPQSDYIRPSLTGKFAGNPWYYGKVTRHQAEMAL NERGHEGDFLIRDSESSPNDFSVSLKAQGKNKHFKVQLKE TVYSIGQRKFSTMEELVEHYKKAPIFTSEQGEKLYLVKHL S | In L1, (KVKRK) replace with GS; Residues 59-78, 84-377, C139S, C266S, C340S |
| L1ΔCT-S2-L2-S3-L3-SH2 | GHMKNSARKASIVKNLKDTLGIGKVKRKGGSAGGSAGGSA MPAYVKFNYMAEREDELSLIKGTKVIVMEKSSDGWWRGSY NGQVGWFPSNYVTEEGDSPLGDHVGSLSEKLAAVVNNLNT GQVLHVVQALYPFSSSNDEELNFEKGDVMDVIEKPENDPE WWKCRKINGMVGLVPKNYVTVMQNNPLTSGLEPSPPQSDY IRPSLTGKFAGNPWYYGKVTRHQAEMALNERGHEGDFLIR DSESSPNDFSVSLKAQGKNKHFKVQLKETVYSIGQRKFST MEELVEHYKKAPIFTSEQGEKLYLVKHLS | di-SH3 construct where 25 C-terminal L1 residues were replaced by a $(GGSA)_3$ linker; Residues 59-83,109-377, C139S, C266S, C340S |

| | | |
|---|---|---|
| L1basic-S2-L2-S3-L3-SH2 | GHMKNSARKASIVKNLKDTLGIGKVKRKPSVPKSASPADK<br>SFVKPGKRLYKLNMPAYVKFNYMAEREDELSLIKGTKVIV<br>MEKSSDGWWRGSYNGQVGWFPSNYVTEEGDSPLGDHVGSL<br>SEKLAAVVNNLNTGQVLHVVQALYPFSSSNDEELNFEKGD<br>VMDVIEKPENDPEWWKCRKINGMVGLVPKNYVTVMQNNPL<br>TSGLEPSPPQSDYIRPSLTGKFAGNPWYYGKVTRHQAEMA<br>LNERGHEGDFLIRDSESSPNDFSVSLKAQGKNKHFKVQLK<br>ETVYSIGQRKFSTMEELVEHYKKAPIFTSEQGEKLYLVKH<br>LS | L1 acidic residues mutated to K's; Residues 59-377, C139S, C266S, C340S |
| L1addcharge-S2-L2-S3-L3-SH2 | GHMKNSARKASRKKNLKRTLGIGKVKRKPSDDDSADDADD<br>SFVDPGERLYDLNMPAYVKFNYMAEREDELSLIKGTKVIV<br>MEKSSDGWWRGSYNGQVGWFPSNYVTEEGDSPLGDHVGSL<br>SEKLAAVVNNLNTGQVLHVVQALYPFSSSNDEELNFEKGD<br>VMDVIEKPENDPEWWKCRKINGMVGLVPKNYVTVMQNNPL<br>TSGLEPSPPQSDYIRPSLTGKFAGNPWYYGKVTRHQAEMA<br>LNERGHEGDFLIRDSESSPNDFSVSLKAQGKNKHFKVQLK<br>ETVYSIGQRKFSTMEELVEHYKKAPIFTSEQGEKLYLVKH<br>LS | Added basic charges to N-term and acidic charges to C-term of linker; Residues 59-377, C139S, C266S, C340S |
| L1D/Rswap-S2-L2-S3-L3-SH2 | GHMKNSARKASIVKNLKRTLGIGKVKRKPSVPDSASPADD<br>SFVDPGEDLYDLNMPAYVKFNYMAEREDELSLIKGTKVIV<br>MEKSSDGWWRGSYNGQVGWFPSNYVTEEGDSPLGDHVGSL<br>SEKLAAVVNNLNTGQVLHVVQALYPFSSSNDEELNFEKGD<br>VMDVIEKPENDPEWWKCRKINGMVGLVPKNYVTVMQNNPL<br>TSGLEPSPPQSDYIRPSLTGKFAGNPWYYGKVTRHQAEMA<br>LNERGHEGDFLIRDSESSPNDFSVSLKAQGKNKHFKVQLK<br>ETVYSIGQRKFSTMEELVEHYKKAPIFTSEQGEKLYLVKH<br>LS | D to R swapped in linker to make N-terminus more basic and C-terminus more acidic; Residues 59-377, C139S, C266S, C340S |
| L1chargeshuffle S2-L2-S3-L3-SH2 | GHMKNSADKASIVDNLKDTLGIGKVDRKPSVPKSASPADR<br>SFVKPGERLYDLNMPAYVKFNYMAEREDELSLIKGTKVIV<br>MEKSSDGWWRGSYNGQVGWFPSNYVTEEGDSPLGDHVGSL<br>SEKLAAVVNNLNTGQVLHVVQALYPFSSSNDEELNFEKGD<br>VMDVIEKPENDPEWWKCRKINGMVGLVPKNYVTVMQNNPL<br>TSGLEPSPPQSDYIRPSLTGKFAGNPWYYGKVTRHQAEMA<br>LNERGHEGDFLIRDSESSPNDFSVSLKAQGKNKHFKVQLK<br>ETVYSIGQRKFSTMEELVEHYKKAPIFTSEQGEKLYLVKH<br>LS | Only the charges in the linker shuffled; Residues 59-377, C139S, C266S, C340S |
| L1c30shuffle-S2-L2-S3-L3-SH2 | GHMKNSARKASIVKNLKDTLGIGPYRDSVPASDSLKSEAF<br>GKDRDKVPPDVLNMPAYVKFNYMAEREDELSLIKGTKVIV<br>MEKSSDGWWRGSYNGQVGWFPSNYVTEEGDSPLGDHVGSL<br>SEKLAAVVNNLNTGQVLHVVQALYPFSSSNDEELNFEKGD<br>VMDVIEKPENDPEWWKCRKINGMVGLVPKNYVTVMQNNPL<br>TSGLEPSPPQSDYIRPSLTGKFAGNPWYYGKVTRHQAEMA<br>LNERGHEGDFLIRDSESSPNDFSVSLKAQGKNKHFKVQLK<br>ETVYSIGQRKFSTMEELVEHYKKAPIFTSEQGEKLYLVKH<br>LS | Linker sequence shuffled keeping a 20 N-terminal residues unchanged; Residues 59-377, C139S, C266S, C340S |

| | | |
|---|---|---|
| Nck(L1ggsa10) | GHMAEEVVVVAKFDYVAQQEQELDIKKNERLWLLDDSKSW<br>WRVRNSMNKTGFVPSNYVERGGSAGGSAGGSAGGSAGGSA<br>GSGGSAGGSAGGSAGGSAGGSAGSDLNMPAYVKFNYMAER<br>EDELSLIKGTKVIVMEKCSDGWWRGSYNGQVGWFPSNYVT<br>EEGDSPLGDHVGSLSEKLAAVVNNLNTGQVLHVVQALYPF<br>SSSNDEELNFEKGDVMDVIEKPENDPEWWKCRKINGMVGL<br>VPKNYVTVMQNNPLTSGLEPSPPQCDYIRPSLTGKFAGNP<br>WYYGKVTRHQAEMALNERGHEGDFLIRDSESSPNDFSVSL<br>KAQGKNKHFKVQLKETVYCIGQRKFSTMEELVEHYKKAPI<br>FTSEQGEKLYLVKHLS | L1 replaced with a GGSA linker in full-length Nck; Residues 1-58, 109-377 |
| Nck ΔL1b | GHMAEEVVVVAKFDYVAQQEQELDIKKNERLWLLDDSKSW<br>WRVRNSMNKTGFVPSNYVERKNSGGSAGGSAGGSATLGIG<br>KVKRKPSVPDSASPADDSFVDPGERLYDLNMPAYVKFNYM<br>AEREDELSLIKGTKVIVMEKCSDGWWRGSYNGQVGWFPSN<br>YVTEEGDSPLGDHVGSLSEKLAAVVNNLNTGQVLHVVQAL<br>YPFSSSNDEELNFEKGDVMDVIEKPENDPEWWKCRKINGM<br>VGLVPKNYVTVMQNNPLTSGLEPSPPQCDYIRPSLTGKFA<br>GNPWYYGKVTRHQAEMALNERGHEGDFLIRDSESSPNDFS<br>VSLKAQGKNKHFKVQLKETVYCIGQRKFSTMEELVEHYKK<br>APIFTSEQGEKLYLVKHLS | N-terminal 15 residues replaced with a GGSA linker, in full-length Nck; Residues 1-60, 74-377 |
| Nck(L1shuffle) | GHMAEEVVVVAKFDYVAQQEQELDIKKNERLWLLDDSKSW<br>WRVRNSMNKTGFVPSNYVERKNSADKASIVDNLKDTLGIG<br>PYRDSVPASRSLKSEAFGKDRDKVPPKVLNMPAYVKFNYM<br>AEREDELSLIKGTKVIVMEKCSDGWWRGSYNGQVGWFPSN<br>YVTEEGDSPLGDHVGSLSEKLAAVVNNLNTGQVLHVVQAL<br>YPFSSSNDEELNFEKGDVMDVIEKPENDPEWWKCRKINGM<br>VGLVPKNYVTVMQNNPLTSGLEPSPPQCDYIRPSLTGKFA<br>GNPWYYGKVTRHQAEMALNERGHEGDFLIRDSESSPNDFS<br>VSLKAQGKNKHFKVQLKETVYCIGQRKFSTMEELVEHYKK<br>APIFTSEQGEKLYLVKHLS | Residues in L1 shuffled in full-length Nck |
| SH3-1 | GHMAEEVVVVAKFDYVAQQEQELDIKKNERLWLLDDSKSW<br>WRVRNSMNKTGFVPSNYVERKNSAR | Residues 1-63 |
| SH3-2 | GHMDLNMPAYVKFNYMAEREDELSLIKGTKVIVMEKSSDG<br>WWRGSYNGQVGWFPSNYVTEEGDSPL | Residues 106-168, C139S |
| SH3-3 | GHMHVVQALYPFSSSNDEELNFEKGDVMDVIEKPENDPEW<br>WKCRKINGMVGLVPKNYVTVMQNNPLTSGL | Residues 193-259 |
| Isolated L1 | GHMKNSARKASIVKNLKDTLGIGKVKRKPSVPDSASPADD<br>SFVDPGERLYDLN | Isolated L1; Residues 59-108 |

| | | |
|---|---|---|
| $(SUMO)_5$-$(SIM)_5$ | GHMGGSWGGSMSEEKPKEGVKTENDHINLKVAGQDGSVVQ<br>FKIKRHTPLSKLMKAYSERQGLSMRQIRFRFDGQPINETD<br>TPAQLEMEDEDTIDVFQQQTVVGGSGGSGGSGGSMSEEKP<br>KEGVKTENDHINLKVAGQDGSVVQFKIKRHTPLSKLMKAY<br>SERQGLSMRQIRFRFDGQPINETDTPAQLEMEDEDTIDVF<br>QQQTVVGGSGGSGGSGGSMSEEKPKEGVKTENDHINLKVA<br>GQDGSVVQFKIKRHTPLSKLMKAYSERQGLSMRQIRFRFD<br>GQPINETDTPAQLEMEDEDTIDVFQQQTVVGGSGGSGGSG<br>GSMSEEKPKEGVKTENDHINLKVAGQDGSVVQFKIKRHTP<br>LSKLMKAYSERQGLSMRQIRFRFDGQPINETDTPAQLEME<br>DEDTIDVFQQQTVVGGSGGSGGSGGSMSEEKPKEGVKTEN<br>DHINLKVAGQDGSVVQFKIKRHTPLSKLMKAYSERQGLSM<br>RQIRFRFDGQPINETDTPAQLEMEDEDTIDVFQQQTVVGG<br>SGGSGGSWGGSKVDVIDLTIESSSDEEEDPPAKRGGSGGS<br>GGSGGSKVDVIDLTIESSSDEEEDPPAKRGGSGGSGGSGG<br>SKVDVIDLTIESSSDEEEDPPAKRGGSGGSGGSGGSKVDV<br>IDLTIESSSDEEEDPPAKRG<br>GSGGSGGSGGSKVDVIDLTIESSSDEEEDPPAKRGGSCGR<br>SENLYFQ | SUMO is the human SUMO-3 isoform. Residues 1-92, C47S.<br>SIM is from PIASx. |
| $(SUMO)_5$-L1chargeshuffle-$(SIM)_5$ | GHMGGSWGGSMSEEKPKEGVKTENDHINLKVAGQDGSVVQ<br>FKIKRHTPLSKLMKAYSERQGLSMRQIRFRFDGQPINETD<br>TPAQLEMEDEDTIDVFQQQTVVGGSGGSGGSGGSMSEEKP<br>KEGVKTENDHINLKVAGQDGSVVQFKIKRHTPLSKLMKAY<br>SERQGLSMRQIRFRFDGQPINETDTPAQLEMEDEDTIDVF<br>QQQTVVGGSGGSGGSGGSMSEEKPKEGVKTENDHINLKVA<br>GQDGSVVQFKIKRHTPLSKLMKAYSERQGLSMRQIRFRFD<br>GQPINETDTPAQLEMEDEDTIDVFQQQTVVGGSGGSGGSG<br>GSMSEEKPKEGVKTENDHINLKVAGQDGSVVQFKIKRHTP<br>LSKLMKAYSERQGLSMRQIRFRFDGQPINETDTPAQLEME<br>DEDTIDVFQQQTVVGGSGGSGGSGGSMSEEKPKEGVKTEN<br>DHINLKVAGQDGSVVQFKIKRHTPLSKLMKAYSERQGLSM<br>RQIRFRFDGQPINETDTPAQLEMEDEDTIDVFQQQTVVGG<br>SGGSKNSADKASIVDNLKDTLGIGKVDRKPSVPKSASPAD<br>RSFVKPGERLYDLNRSGGSWGGSKVDVIDLTIESSSDEEE<br>DPPAKRGGSGGSGGSGGSKVDVIDLTIESSSDEEEDPPAK<br>RGGSGGSGGSGGSKVDVIDLTIESSSDEEEDPPAKRGGSG<br>GSGGSGGSKVDVIDLTIESSSDEEEDPPAKRGGSGGSGGS<br>GGSKVDVIDLTIESSSDEEEDPPAKRGGSCGRSENLYFQ | L1chargeshuffle added to $(SUMO)_5$-$(SIM)_5$ |

| | | |
|---|---|---|
| $(SUMO)_5$-L1-$(SIM)_5$ | GHMGGSWGGSMSEEKPKEGVKTENDHINLKVAGQDGSVVQ<br>FKIKRHTPLSKLMKAYSERQGLSMRQIRFRFDGQPINETD<br>TPAQLEMEDEDTIDVFQQQTVVGGSGGSGGSGGSMSEEKP<br>KEGVKTENDHINLKVAGQDGSVVQFKIKRHTPLSKLMKAY<br>SERQGLSMRQIRFRFDGQPINETDTPAQLEMEDEDTIDVF<br>QQQTVVGGSGGSGGSGGSMSEEKPKEGVKTENDHINLKVA<br>GQDGSVVQFKIKRHTPLSKLMKAYSERQGLSMRQIRFRFD<br>GQPINETDTPAQLEMEDEDTIDVFQQQTVVGGSGGSGGSG<br>GSMSEEKPKEGVKTENDHINLKVAGQDGSVVQFKIKRHTP<br>LSKLMKAYSERQGLSMRQIRFRFDGQPINETDTPAQLEME<br>DEDTIDVFQQQTVVGGSGGSGGSGGSMSEEKPKEGVKTEN<br>DHINLKVAGQDGSVVQFKIKRHTPLSKLMKAYSERQGLSM<br>RQIRFRFDGQPINETDTPAQLEMEDEDTIDVFQQQTVVGG<br>SGGSKNSARKASIVKNLKDTLGIGKVKRKPSVPDSASPAD<br>DSFVDPGERLYDLNRSGGSWGGSKVDVIDLTIESSSDEEE<br>DPPAKRGGSGGSGGSGGSKVDVIDLTIESSSDEEEDPPAK<br>RGGSGGSGGSGGSKVDVIDLTIESSSDEEEDPPAKRGGSG<br>GSGGSGGSKVDVIDLTIESSSDEEEDPPAKRGGSGGSGGS<br>GGSKVDVIDLTIESSSDEEEDPPAKRGGSCGRSENLYFQ | |
| L1-S2 | GHMKNSARKASIVKNLKDTLGIGKVKRKPSVPDSASPADD<br>SFVDPGERLYDLNMPAYVKFNYMAEREDELSLIKGTKVIV<br>MEKSSDGWWRGSYNGQVGWFPSNYVTEEGDSPL | Residues 59-168, C139S |
| L1-S3 | GHMKNSARKASIVKNLKDTLGIGKVKRKPSVPDSASPADD<br>SFVDPGERLYDLNVLHVVQALYPFSSSNDEELNFEKGDVM<br>DVIEKPENDPEWWKCRKINGMVGLVPKN<br>YVTVMQNNPLTSGL | Residues 59-108, 191-259 |
| PRM-1 | WGGSLRRQAPPPPPPS | |
| PRM-2 | WGGSAPPPPPPSRGG | |
| PRM-3 | WGGSRGGPPPPPPPPH | |
| PRM-4 | WGGSGPPPPPARGRGA | |
| PRM-5 | WGGSARGRGAGAPPPPPS | |
| PRM-6 | WGGSGAPPPPPSRAPT | |
| PRM-7 | WGGSTAAPPPPPPSRP | |
| PRM-8 | WGGSVAVPPPPPNRMY | |
| PRM-9 | WGGSNRMYPPPPPALP | |
| PRM-10 | WGGSSAPSGPPPPPPSVL | |
| PRM-11 | WGGSVAPPPPPPPPPPG | |

| | | |
|---|---|---|
| PRM-12 | WGGSPGPPPPPGLPSD | |
| di-PRM-1 | WGGSLRRQAPPPPPPSRGGPPPPPPPPH | |
| di-PRM-2 | WGGSGPPPPPARGRGAPPPPPSRAP | |
| di-PRM-3 | WGGSVPPPPPNRMYPPPPPALPS | |

**Table S2. Purification summary of the various Nck constructs:**

| **Construct** | **Step/Columns** |
|---|---|
| S1-L1-S2-L3-SH2 | GST (pH 8), TEV cleavage, Source15S (pH7.0, elutes ~ 170 mM NaCl), SD200 |
| S1-L1-S3-L3-SH2 | GST (pH 8), TEV cleavage, Source15S (pH 7.0, elutes ~ 130 mM NaCl), SD200 |
| S2-L2-S3-L3-SH2 | GST (pH 8), TEV cleavage, Source15Q (pH 7.0, elutes ~ 90 mM NaCl, SD200 |
| L1-S2-L2-S3-L3-SH2 | GST (pH 8), TEV cleavage, Source15Q (pH 7.0, elutes ~ 80 mM NaCl), SD200 |
| L1chargeshuffle S2-L2-S3-L3-SH2 | GST (pH 8), TEV cleavage, Source15Q (pH 8.0, elutes ~ 80 mM NaCl), SD200 |
| L1non-chargeshuffle-S2-L2-S3-L3-SH2 | GST (pH 8), TEV cleavage, Source15Q (pH 7.0, elutes ~ 90 mM NaCl), SD200 |
| ΔL1-S2-L2-S3-L3-SH2 | GST (pH 8), TEV cleavage, Source15Q (pH 7.0, elutes ~ 90 mM NaCl), SD200 |
| L1ΔCT-S2-L2-S3-L3-SH2 | GST (pH 8), TEV cleavage, Source15Q (pH 8.0, elutes ~ 60 mM NaCl), SD200 |
| L1Δ(KVKRK)-S2-L2-S3-L3-SH2 | GST (pH 8), TEV cleavage, Source15Q (pH 7.0, elutes ~ 100 mM NaCl), SD200 |
| L1basic-S2-L2-S3-L3-SH2 | GST (pH 8), TEV cleavage, precipitates at low salt after cleavage, raise salt to 200 KCl, Source15S (pH 7.0, elutes ~ broadly 250 - 290 mM NaCl), SD200 |
| L1K/E S2-L2-S3-L3-SH2 | GST (pH 8), TEV cleavage, Source15Q (pH 7.0, elutes ~ 130 mM NaCl), SD200 |

| | |
|---|---|
| L1D/Rswap-S2-L2-S3-L3-SH2 | GST (pH 8), TEV cleavage, Source15S (pH 7.0, elutes ~ 200 mM NaCl), SD200 |
| Nck(L1ggsa) | GST (pH 8), TEV cleavage, Source15Q (pH 7.0, elutes ~ 110 mM NaCl, SD200) |
| Nck ΔL1b | GST (pH 8), TEV cleavage, Source15Q (pH 7.0, elutes ~ 110 mM NaCl, SD200 |
| Nck(L1shuffle) | GST (pH 8), TEV cleavage, Source15Q (pH 7.0, elutes ~ 70 mM NaCl), SD200 |
| Isolated L1 WT | Amylose (pH 8), TEV cleavage, Source15S (pH 7, elutes 250 mM NaCl), SD200 |

**Phase Separation of SUMO-SIM proteins**

96 well, untreated plates from Corning were blocked with 3% BSA for 1 hr at room temperature. Wells were then washed with deionized water three times and dried with argon gas. Concentrated protein stocks $(SUMO)_5$-$SIM_5$ and $(SUMO)_5$-L1-$(SIM)_5$ (both in 10 mM tris pH 8, 50 mM NaCl), were diluted to appropriate concentrations in 10 mM tris pH 8, 50 mM NaCl, to up to 90 µL. 10 µL of 1 M Imidazole pH 7, 1.05 M NaCl were added to induce phase separation (bringing final buffer condition to 100 mM Imidazole pH 7 and 150 mM NaCl. Wells were covered to prevent evaporation and left at room temperature for 22 hrs, after which they were imaged under a light microscope.

**Peptide Synthesis**

PRM peptides were synthesized at the UTSW proteomics center. To facilitate absorbance measurements and concentration determination, a tryptophan a WGGS linker) was added at the N-terminus of the peptides. Peptide sequences are indicated in Fig. 3.

**Atomistic simulations**

All simulations were performed using the CAMPARI modeling suite (http://campari.sourceforge.net). The simulations deploy the ABSINTH implicit solvent model and forcefield paradigm (4). In this model, the polypeptide atoms and mobile solution ions are modeled in atomic detail whereas the solvent treated using a mean field model that provides an estimate of the free energy of solvation by bootstrapping against known experimental data for model compounds and accounting for many-body effects that lead to spatial dielectric inhomogeneities. The dielectric constant for water was set to 78 and the simulation temperature used was 298 K. The simulations utilize the parameters from the abs_3.2_opls.prm parameter file for the interactions of polypeptide atoms and the parameters of Mao and Pappu (5) for the solution $Na^+$ and $Cl^-$ ions. The tethered Ac-L1-S2-Nme system was enclosed in a droplet of radius 100Å and excess $Na^+$ and $Cl^-$ ions were included to mimic a salt concentration of 15 mM. Spherical cutoffs of 10 and 14 Å, respectively were used to truncate and taper the Lennard-Jones and electrostatic interactions. For electrostatic interactions, these cutoffs were applied only for interactions between residues that lack an excess charge. In contrast, no cutoffs

were applied in the calculation of electrostatic interactions between pairs of residues where at least one of the residues has a net charge. We performed ten independent Hamiltonian Switch-Metropolis Monte Carlo (HS-MMC) simulations (6) for the L1-S2 system. This method enables efficient sampling of intrinsically disordered regions that are tethered to ordered domains. Each simulation was initiated from an entirely different starting conformation for the L1 linker and the initial coordinates for the S2 domain were drawn from the protein data bank (PDB: 2JS0). For each run, we sampled conformational space using a total of $8\times10^7$ moves and of these, $5\times10^6$ of the moves were discarded as equilibration. Across ten independent simulations we obtain close to $10^9$ independent equilibrium samples of conformational space. When converted to the currency of molecular dynamics simulations, the aggregate simulation time is on the order of several microseconds. The move sets for the Monte Carlo simulations combine pivots, concerted rotations, sidechain rotations, mutual reorientations and displacements of the two domains with respect to each other, translations of the mobile ions, and a series of moves that enable the efficient sampling of the conformational degrees of freedom coupled to proline ring systems (7). In addition, the HS-MMC simulations incorporate an auxiliary Markov chain that is introduced with a probability of 0.005 and the number of steps for this auxiliary sampler range from 25 to 75 steps. The details of the HS-MMC approach have been previously published (6).

## SI Appendix References


1. Banjade S & Rosen MK (2014) Phase transitions of multivalent proteins can promote clustering of membrane receptors. *eLife* 3: e04123.
2. Li P*, et al.* (2012) Phase transitions in the assembly of multivalent signalling proteins. *Nature* 483(7389):336-340.
3. Doolittle LK, Rosen MK, & Padrick SB (2013) Measurement and analysis of in vitro actin polymerization. *Methods Mol Biol* 1046:273-293.
4. Vitalis A & Pappu RV (2009) ABSINTH: a new continuum solvation model for simulations of polypeptides in aqueous solutions. *J Comput Chem* 30(5):673-699.
5. Mao AH & Pappu RV (2012) Crystal lattice properties fully determine short-range interaction parameters for alkali and halide ions. *J Chem Phys* 137(6):064104.
6. Mittal A, Lyle N, Harmon TS, & Pappu RV (2014) Hamiltonian Switch Metropolis Monte Carlo Simulations for Improved Conformational Sampling of Intrinsically Disordered Regions Tethered to Ordered Domains of Proteins. *J Chem Theory Comput* 10(8):3550-3562.
7. Radhakrishnan A, Vitalis A, Mao AH, Steffen AT, & Pappu RV (2012) Improved atomistic Monte Carlo simulations demonstrate that poly-L-proline adopts heterogeneous ensembles of conformations of semi-rigid segments interrupted by kinks. *J Phys Chem B* 116(23):6862-6871.


## SI Appendix Figure Legends

**Figure S1. Di-valent Nck SH3 proteins do not phase separate equally.** Bright-field microscope images showing the formation of droplets as a concentration of the different proteins indicated on the left. These data are represented as red dots for phase separation and blue dots for absence of phase separation in Fig. 2. Scale bar is 100 μm.

**Figure S2. Basic region of L1 promotes phase separation of di-SH3 Nck constructs.** (a) Sequence of L1 elements in L1-S2-L2-S3-L3-SH2 constructs used in panels (b)-(f). (b)-(f) Phase separation experiments were performed with the indicated di-SH3 proteins and N-WASP, in the presence of 7.5 μM p-Nephrin. Red and blue symbols indicate phase separation and no phase separation, respectively.

**Figure S3. L1 affects phase separation of full-length Nck proteins.** (a) Sequence of L1 elements in full length Nck constructs used in panels (b)-(f). (b-f) Phase separation experiments with Nck constructs in the presence of N-WASP and 7.5 μM p-Nephrin. Red and blue symbols indicate phase separation and no phase separation, respectively.

**Figure S4. Summary of L1 mutations used in the di-SH3 constructs.** The minimum concentration at which phase separation of each construct was observed is listed.

**Figure S5. Effect of L1 is general among different proteins, possibly through electrostatic interactions.** Phase separation experiments with Nck constructs in the presence of N-WASP without Nephrin, for a) Nck and b) NckL1ggsa10. Red and blue symbols indicate phase separation and no phase separation, respectively. (c) Diffusion coefficients obtained from dynamic light scattering

measurements of L1-S2-L2-S3-L3-SH2 (blue circles) and L1chargeshuffle-S2-L2-S3-L3-SH2 (red circles) at different KCl concentrations. (d) Phase separation (red dots) or no phase separation (blue dots) observed using $SUMO_5$-$SIM_5$, $SUMO_5$-L1-$SIM_5$, and $SUMO_5$-L1chargeshuffle-$SIM_5$ proteins.

**Figure S6. L1 binds to regions of S2.** (a) $^{1}H$-$^{15}N$ TROSY spectra of 250 μM L1-S2-L2-S3-L3-SH2 (black), 250 μM S2-L2-S3-L3-SH2 (red) and 310 μM S2-L2-S3-L3-SH2 (blue). Boxes indicate resonances in the L1-S2-L2-S3-L3-SH2 spectrum that have no counterparts in the S2-L2-S3-L3-SH2 spectrum, and thus represent amides in L1. Green boxes indicate crosspeaks assigned to the indicated residues in L1 (bold text); magenta boxes indicate unassigned resonances from L1. Non-bold text indicates assignments for crosspeaks that shift between L1-S2-L2-S3-L3-SH2 and S2-L2-S3-L3-SH2. Lines connect likely counterpart peaks in the two spectra. Unassigned crosspeaks that shift between the two spectra are circled and indicated with NA. (b) Peak intensities for L1 in a $^{1}H/^{15}N$ HSQC spectum of the L1-S2 protein. Residues without bars are unassigned, and are denoted by bold letters.

**Figure S7. L1 binds to regions of S2.** (a) Chemical shift perturbation values for residues of S2 upon deletion of L1 from the L1-S2 protein (top), showing L1-S2 interaction in cis, and upon titration of L1 peptide into S2 (bottom), showing interaction in trans. CSPs in cis were obtained by comparing $^{15}N$ HSQC spectra of

1 mM L1-S2 and 1 mM S2. Trans CSPs were obtained comparing spectra of 500 μM S2 with 2.5 mM L1 + 450 μM S2. Asterisks denote broadened residues upon L1 binding. (b) Second Nck SH3 domain structure (PDB ID 2JS0) indicating regions of the domain that show changes in chemical shift upon interaction with L1 in cis (top) and in trans (bottom). Orange coloring code denotes amides that have CSP > 0.05 ppm and those that have broadened completely (asterisks). A PRM peptide taken from the structure of the Grb2 C-terminal SH3 domain (aligned with the Nck SH3 domain) and its proline-rich peptide ligand (PDB 1IO6) is shown as green sticks. (c) Electrostatic surface potential of S2 as calculated using the APBS plugin in Pymol.

**Figure S8. L1 can bind in trans and its effect is observed in various contexts.** (b) $^{1}H/^{15}N$ HSQC spectra of S2 in the presence of 0 μM, 250 μM, 750 μM, 1000 μM, 1500 μM, 2000 μM and 2450 μM L1 peptide. The initial concentration of S2 was 500 μM and the final concentration was 445 μM. (c) (Left panel) Chemical shift changes in D123 amide upon addition of L1 (light orange to dark orange denote an increase in L1 concentration). Right panel shows the corresponding quantification of $K_d$ using the change in chemical shift in D123 upon addition of L1. (a) Overlaid $^{1}H/^{15}N$ HSQC spectra of 300 μM L1-S3 and 300 μM S3 proteins.

**Figure S9. Summary of results from atomistic simulations.** Panel (a) shows the ensemble-averaged distances between pairs of residues within L1 and

between L1 and S2. We calculated these distances from simulations of the L1-S2 system. For each conformation drawn from the equilibrated ensemble at a simulation temperature of 298 K we calculated an inter-residue distance as $R_{ij} = \frac{1}{n_i n_j} \sum_{k=1}^{n_i} \sum_{l=1}^{n_j} \left| \mathbf{r}_k^i - \mathbf{r}_l^j \right|$. Here, $n_i$ and $n_j$ denote the number of atoms within residues *i* and *j*, respectively. The inter-residue distances are calculated by averaging over all conformations drawn from the equilibrium ensemble and is reported in the plot as an ensemble-averaged value for each pair of residues *i* and *j*. The hotter colors correspond to shorter distances and the cooler colors correspond to larger distances. Panel (b) quantifies the inter-domain contacts that form between L1 and S2. Specifically, we quantified the probabilities of forming inter-residue contacts between the residues of L1 and S2. We define an inter-residue contact if at least one pair of non-hydrogen atoms between the residues is within 3.5Å. These contacts are concentrated among residues corresponding to the N-terminal half of L1 and the acidic surface of S2. The only other prominent contacts we observe are due to the tethering of the C-terminal end of L1 at the N-terminal end of S2. The color map for the checkerboard plot is as follows: Cells corresponding to pairs of residues with <1% contact probability are shown in white; those with 1-50% contact probability range from red to blue, and those with >50% contact probability are in black. Panel (c) shows a representative conformation that was drawn from the simulated ensemble to illustrate the types of contacts that can form, albeit with very low overall likelihood – between 1 and 5% as shown in panel (a). The residues of the RT loop are colored in yellow. The sequence stretch of S2 that corresponds

to RGSYNGQVG is colored in purple. The N-terminal half of the backbone of L1 is colored in blue and the C-terminal half in red. Stick representations are used to depict residues of L1 and S2 that are within 5 Å of another residue on the apposing domain. In addition, we used stick representations to depict the Trp and Phe residues of S2 that are spatially proximal to the region that is impacted by the interactions with the L1 linker.

**Figure S10: Histograms of residue-specific interdomain contacts between S2 and L1.** Panel (a) shows percent frequency of interdomain contacts involving residues along S2 and panel (b) the corresponding statistics involving residues along the sequence of L1. The main contacts involve residues from the N-terminal half of L1. Residues on the surface of S2, including those in the vicinity of the RT loop, make contacts with residues of L1.

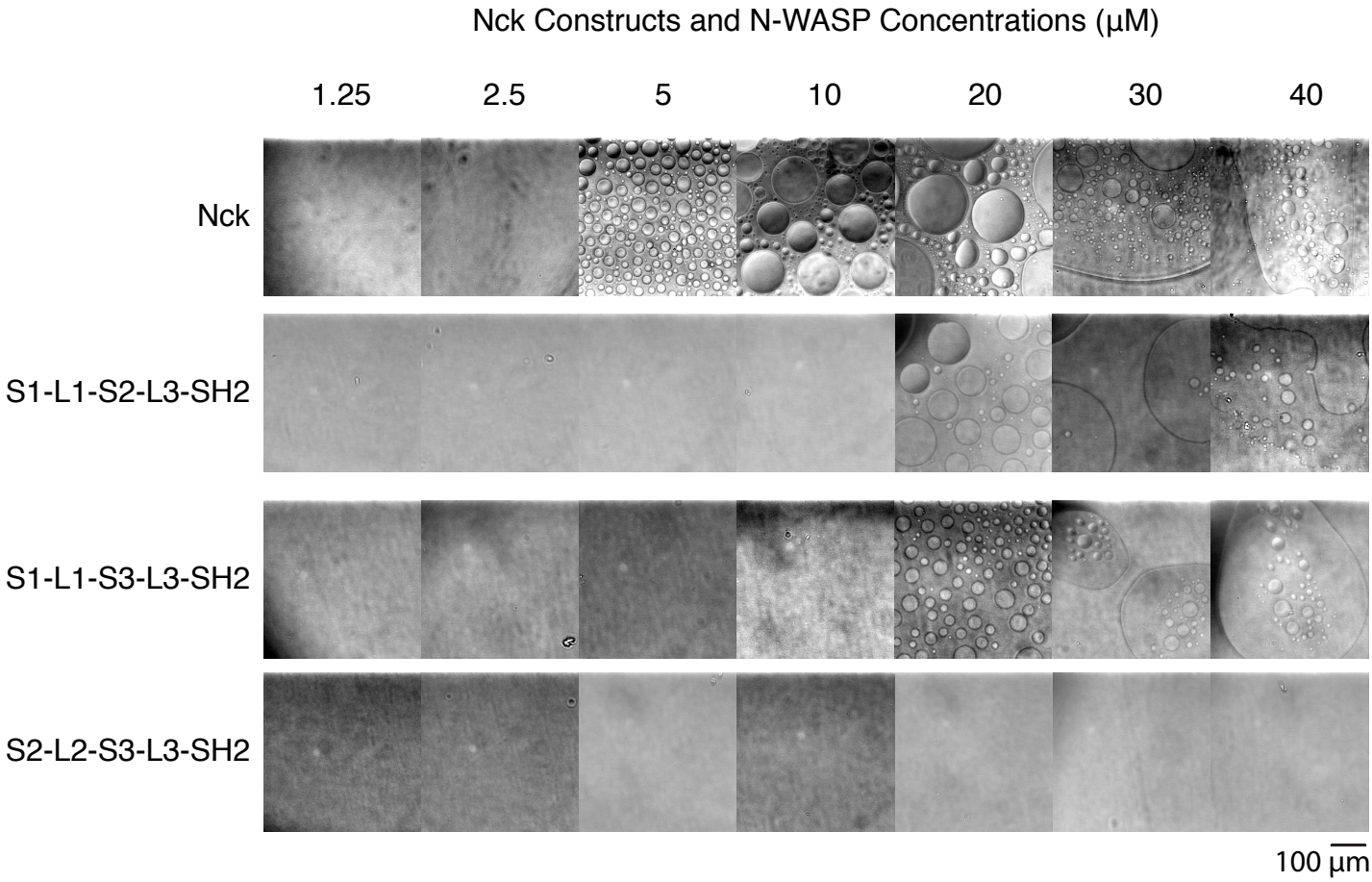
Nck Constructs and N-WASP Concentrations (μM)
1.25
2.5
5
10
20
30
40
Nck
S1-L1-S2-L3-SH2
S1-L1-S3-L3-SH2
S2-L2-S3-L3-SH2
100 μm

# Figure S1

a.

| | |
|---|---|
| L1 (wild-type) | KNSARKASIVKNLKDTLGIGKVKRKPSVPDSASPADDSFVDPGERLYDLN |
| L1basic | KNSARKASIVKNLKDTLGIGKVKRKPSVPKSASPADKSFVKPGKRLYKLN |
| L1addcharge | KNSARKASRKKNLKRTLGIGKVKRKPSDDDSADDADDSFVDPGERLYDLN |
| L1D/R | KNSARKASIVKNLKRTLGIGKVKRKPSVPDSASPADDSFVDPGEDLYDLN |
| L1chargeshuffle | KNSADKASIVDNLKDTLGIGKVDRKPSVPKSASPADRSFVKPGERLYDLN |
| L1c30shuffle | KNSARKASIVKNLKDTLGIGPYRDSVPASDSLKSEAFGKDRDKVPPDVLN |

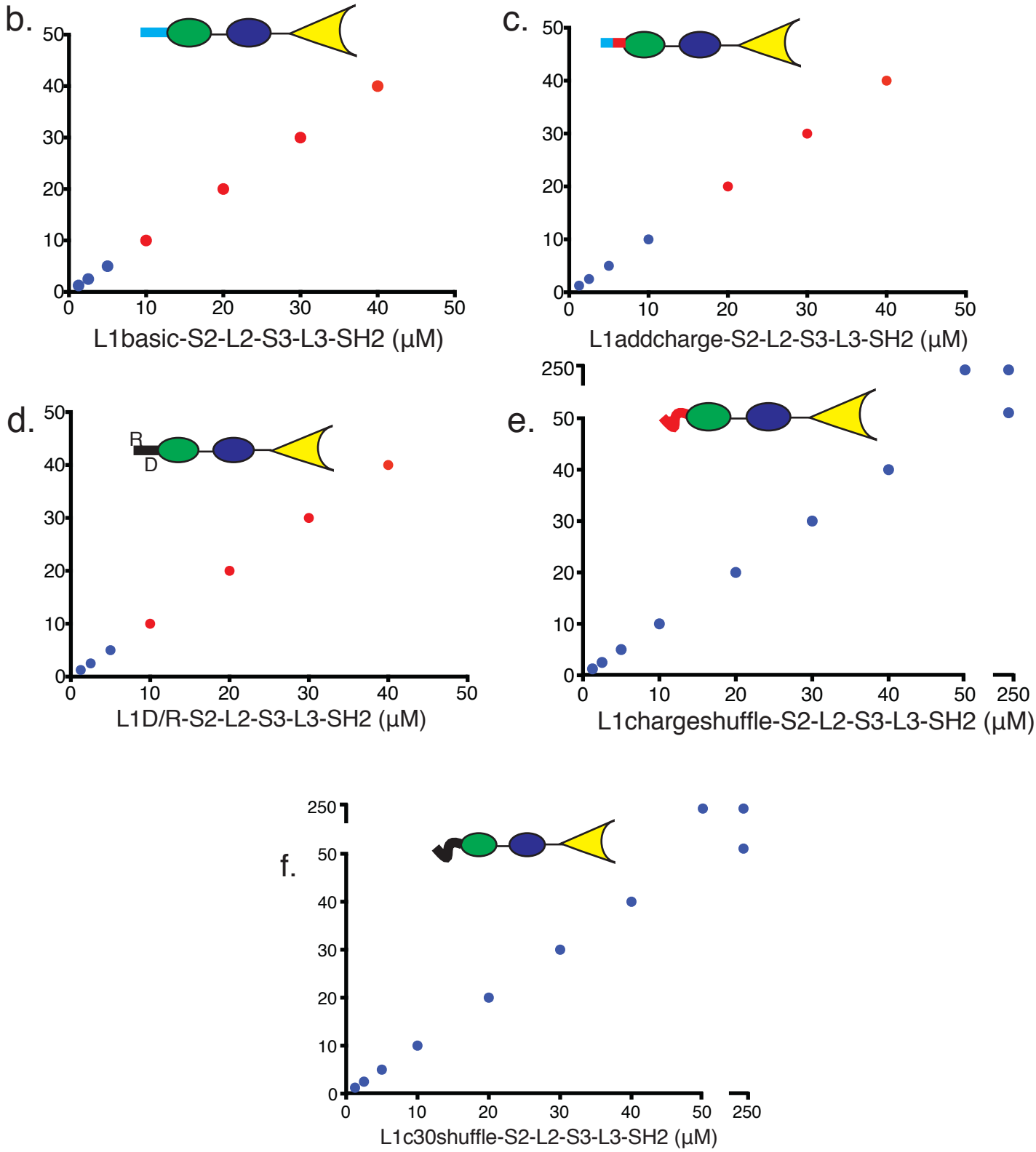


Figure S2

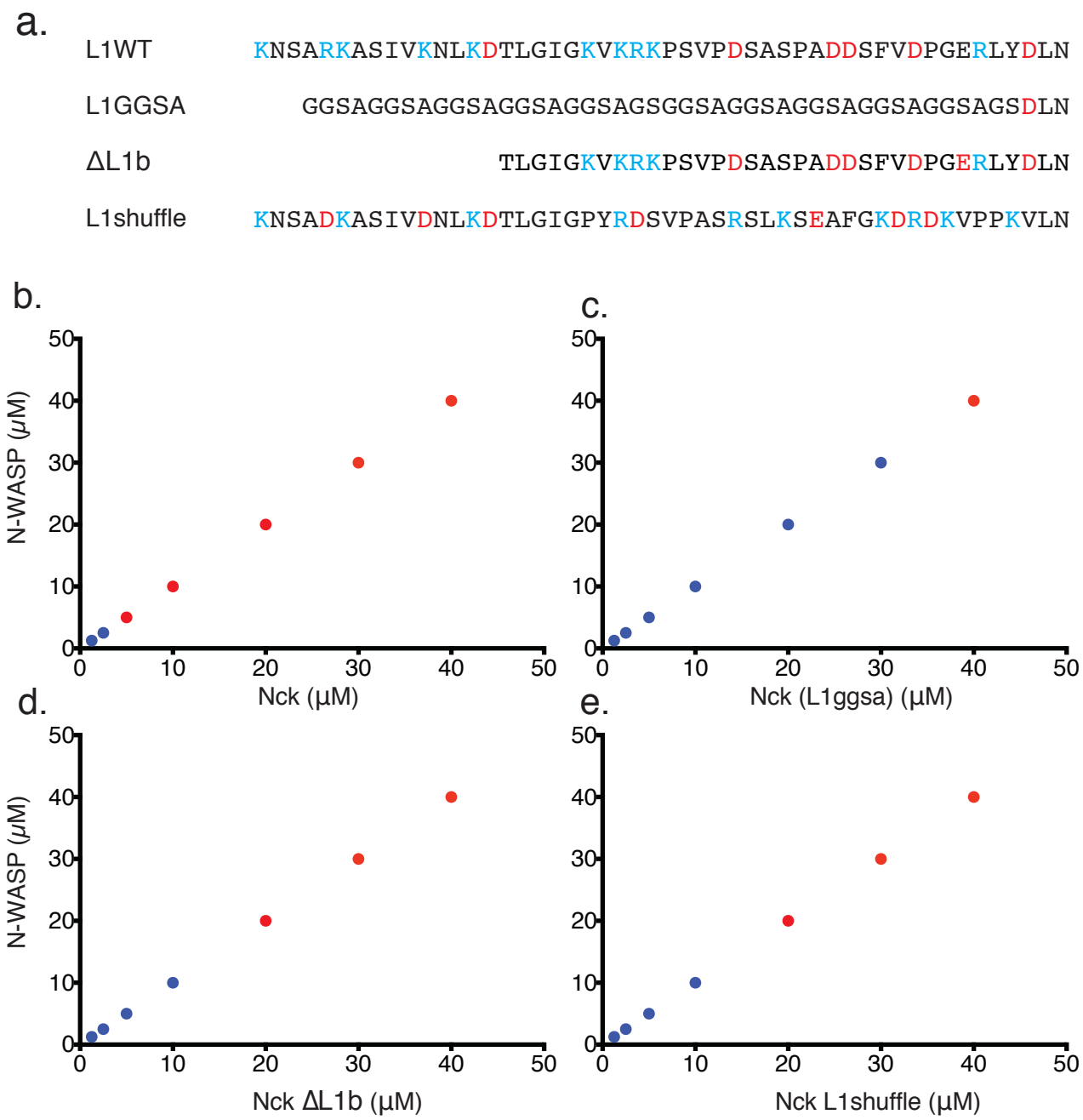
a.
L1WT KNSARKASIVKNLKDTLGIGKVKRKPSVPDSASPADDSFVDPGERLYDLN
L1GGSA GGSAGGSAGGSAGGSAGGSAGSGGSAGGSAGGSAGGSAGGSAGSDLN
ΔL1b TLGIGKVKRKPSVPDSASPADDSFVDPGERLYDLN
L1shuffle KNSADKASIVDNLKDTLGIGPYRDSVPASRSLKSEAFGKDRDKVPPKVLN
b.
N-WASP (μM)
Nck (μM)
c.
Nck (L1ggsa) (μM)
d.
Nck ΔL1b (μM)
e.
Nck L1shuffle (μM)
0
10
20
30
40
50

# Figure S3

| Construct | Sequence | Note | Phase Separation Concentration |
|---|---|---|---|
| L1 (wild-type) | KNSARKASIVKNLKDTLGIGKVKRKPSVPDSASPADDSFVDPGERLYDLN | WT | 30 μM |
| ΔL1 | GIGKVKRKPSVPDSASPADDSFVDPGERLYDLN | delete N-term 20 AA | >250 μM |
| L1KtoE | KNSAREASIVENLEDTLGIGKVKRKPSVPDSASPADDSFVDPGERLYDLN | mutate three N-term **K's** to **E's** | >250 μM |
| L1(ΔKVKRK) | KNSARKASIVKNLKDTLGIG--PSVPDSASPADDSFVDPGERLYDLN | delete KVKRK | >250 μM |
| L1ΔCT | KNSARKASIVKNLKDTLGIGKVKRKGGSAGGSAGGSA | replace C-term 25 AA with $(GGSA)_3$ | 30 μM |
| L1basic | KNSARKASIVKNLKDTLGIGKVKRKPSVPKSASPADKSFVKPGKRLYKLN | mutate C term **acidic's** to **K**'s | 10 μM |
| L1addcharge | KNSARKASRKKNLKRTLGIGKVKRKPSDDDSADDADDSFVDPGERLYDLN | add basic residues N-term and acidic residues C-term | 20 μM |
| L1D/R | KNSARKASIVKNLKRTLGIGKVKRKPSVPDSASPADDSFVDPGEDLYDLN | swap N-term **D** with C-term **R** | 10 μM |
| L1charge-shuffle | KNSADKASIVDNLKDTLGIGKVDRKPSVPKSASPADRSFVKPGERLYDLN | shuffle only charged residues | >250 μM |
| L1c30shuffle | KNSARKASIVKNLKDTLGIGPYRDSVPASDSLKSEAFGKDRDKVPPDVLN | shuffle C-term 30 AA | >250 μM |

# Figure S4

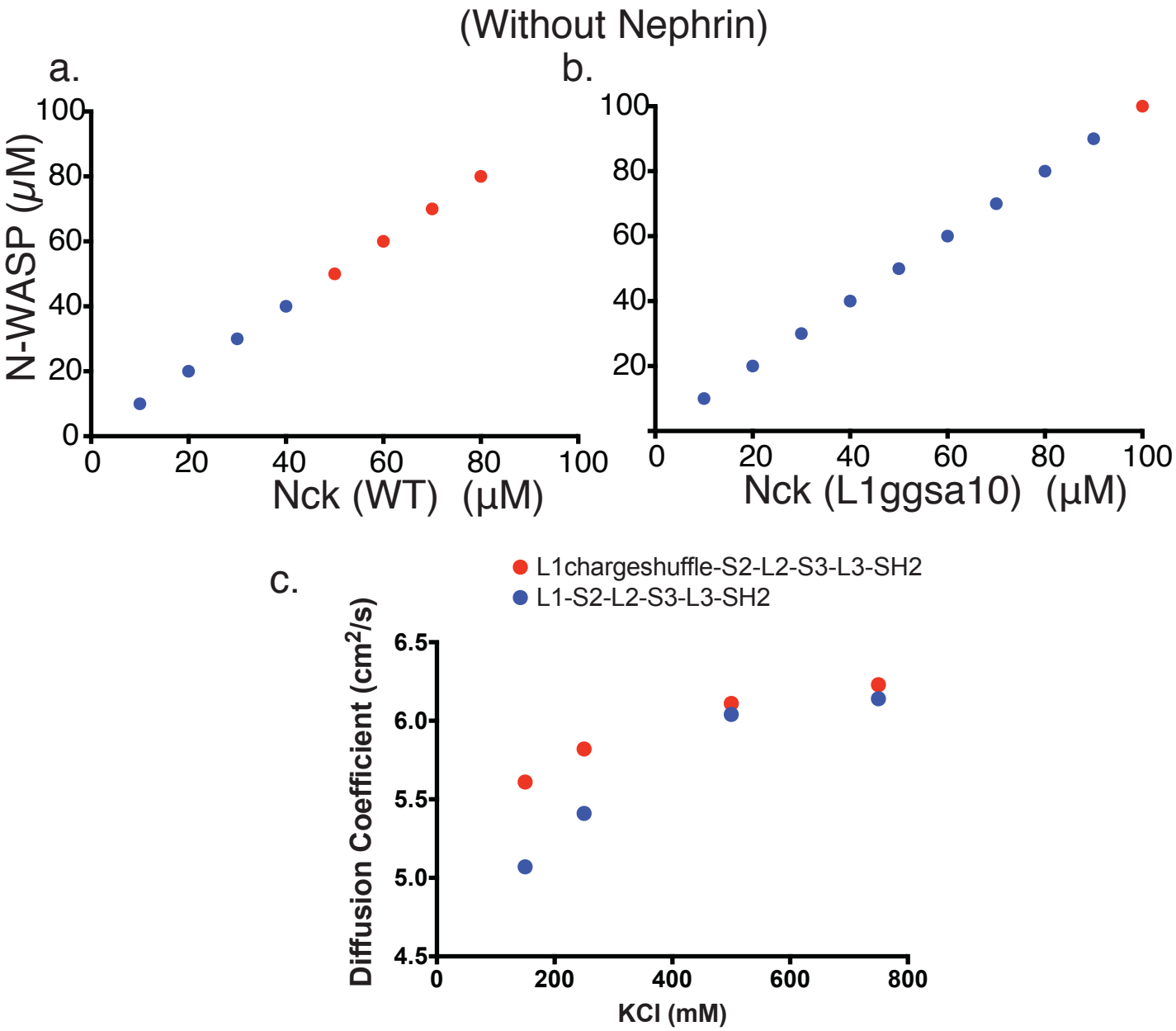
(Without Nephrin)
a.
b.
N-WASP (μM)
Nck (WT) (μM)
Nck (L1ggsa10) (μM)
c.
L1chargeshuffle-S2-L2-S3-L3-SH2
L1-S2-L2-S3-L3-SH2
Diffusion Coefficient (cm²/s)
KCl (mM)
d.
Concentration (μM) 2 4 6 8 10 12
SUMO5-SIM5
SUMO5-L1-SIM5
SUMO5-L1chargeshuffle-SIM5
Phase Separation
No Phase Separation

# Figure S5

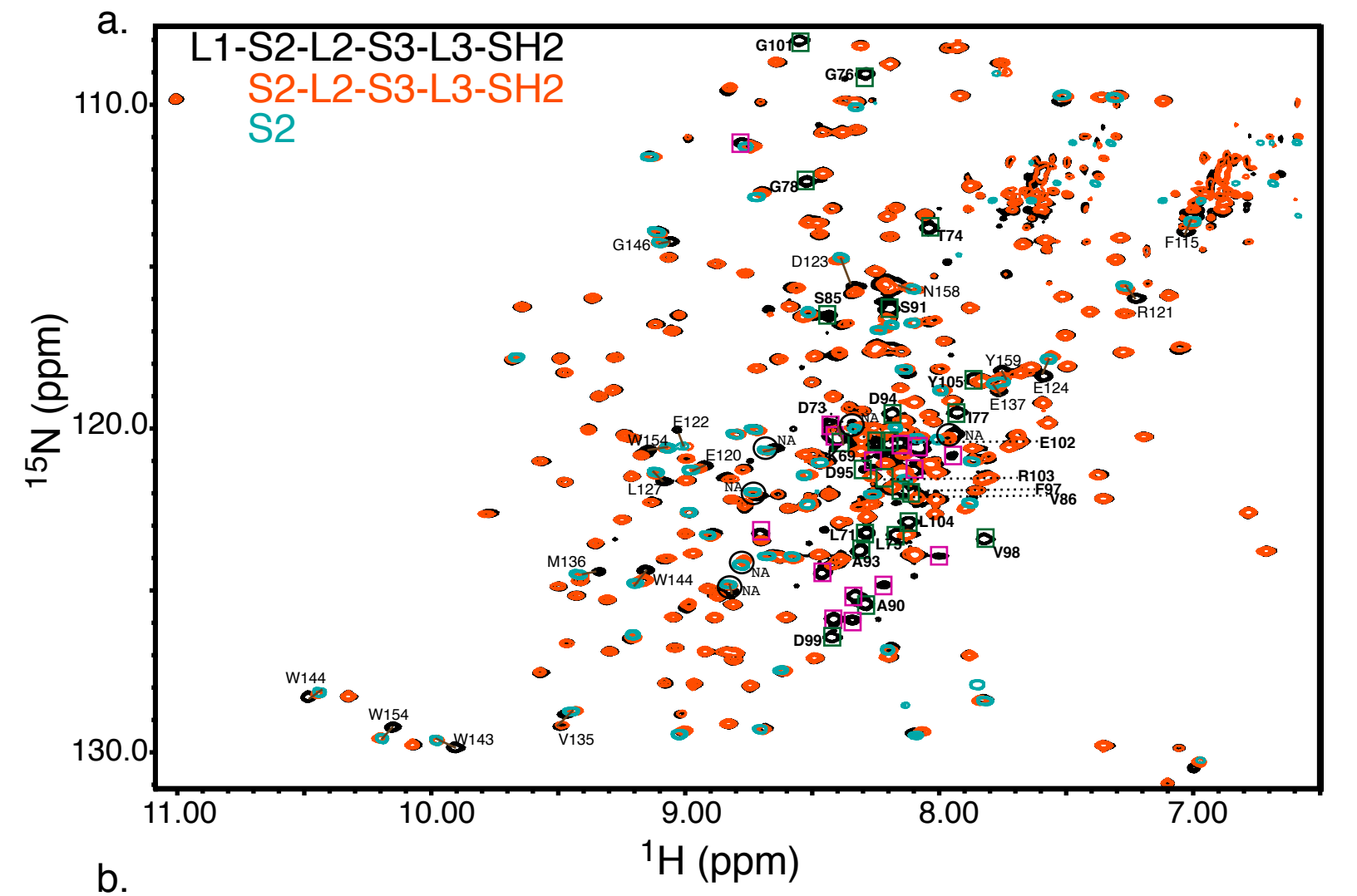


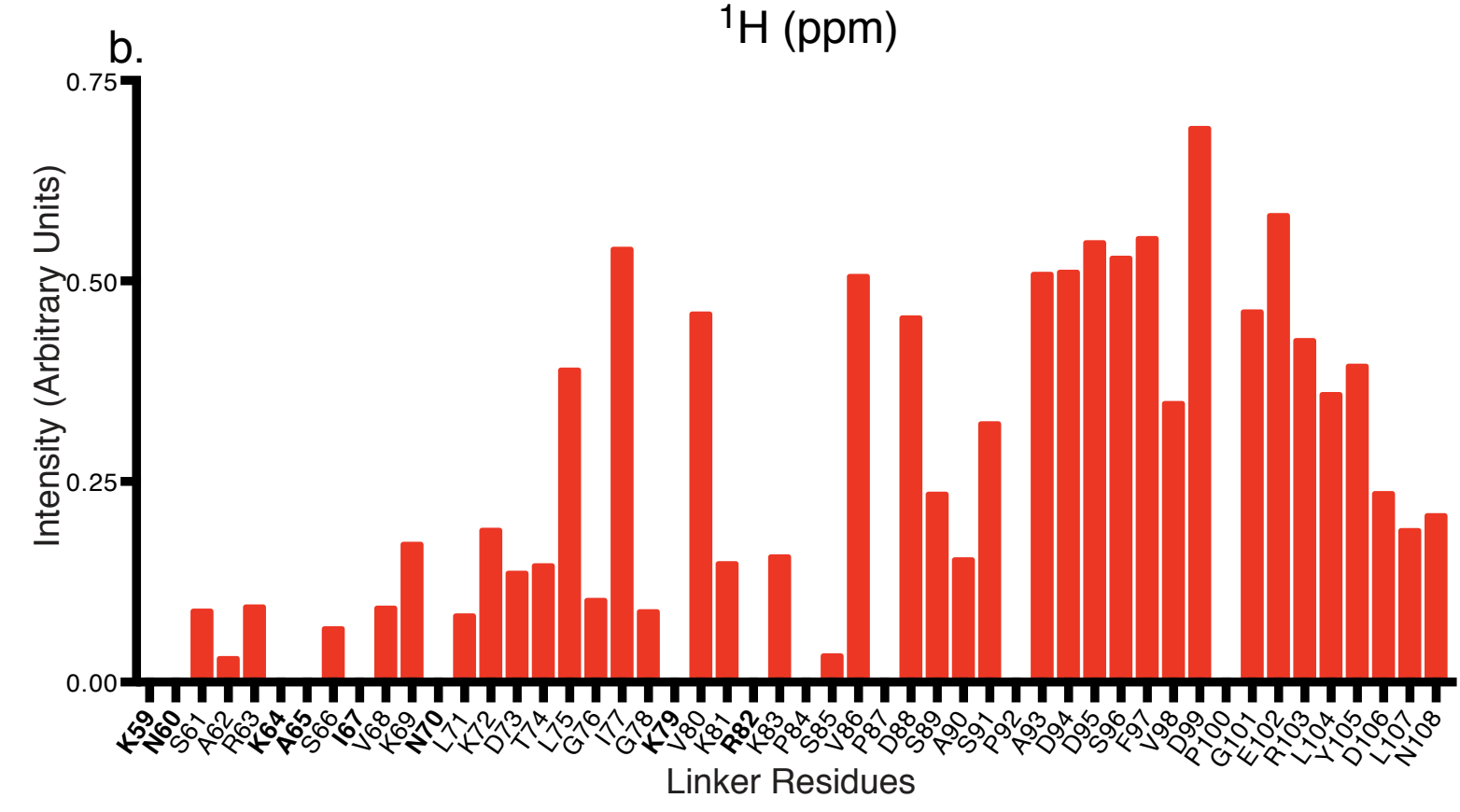


**(Bold = Missing peaks or assignments that are not prolines)**

# Figure S6

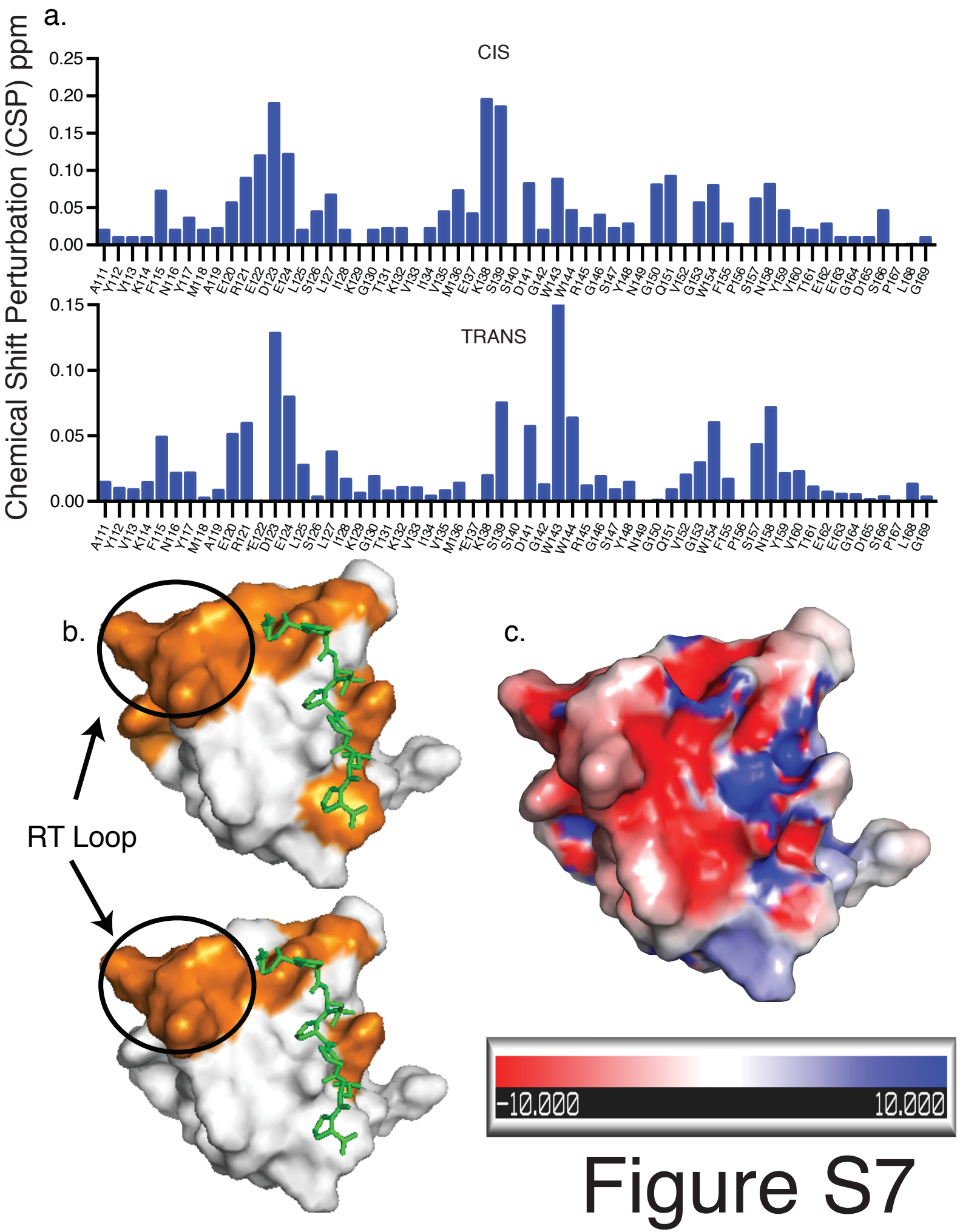
a.
Chemical Shift Perturbation (CSP) ppm
CIS
TRANS
0.25
0.20
0.15
0.10
0.05
0.00
A111 Y112 V113 K114 F115 N116 Y117 M118 A119 E120 R121 E122 D123 E124 L125 S126 L127 I128 K129 G130 T131 K132 V133 I134 V135 M136 E137 K138 S139 S140 D141 G142 W143 W144 R145 G146 S147 Y148 N149 G150 Q151 V152 G153 W154 F155 P156 S157 N158 Y159 V160 T161 E162 E163 G164 D165 S166 P167 L168 G169
*E122 *E137
b.
RT Loop
c.
-10.000
10.000

Figure S7

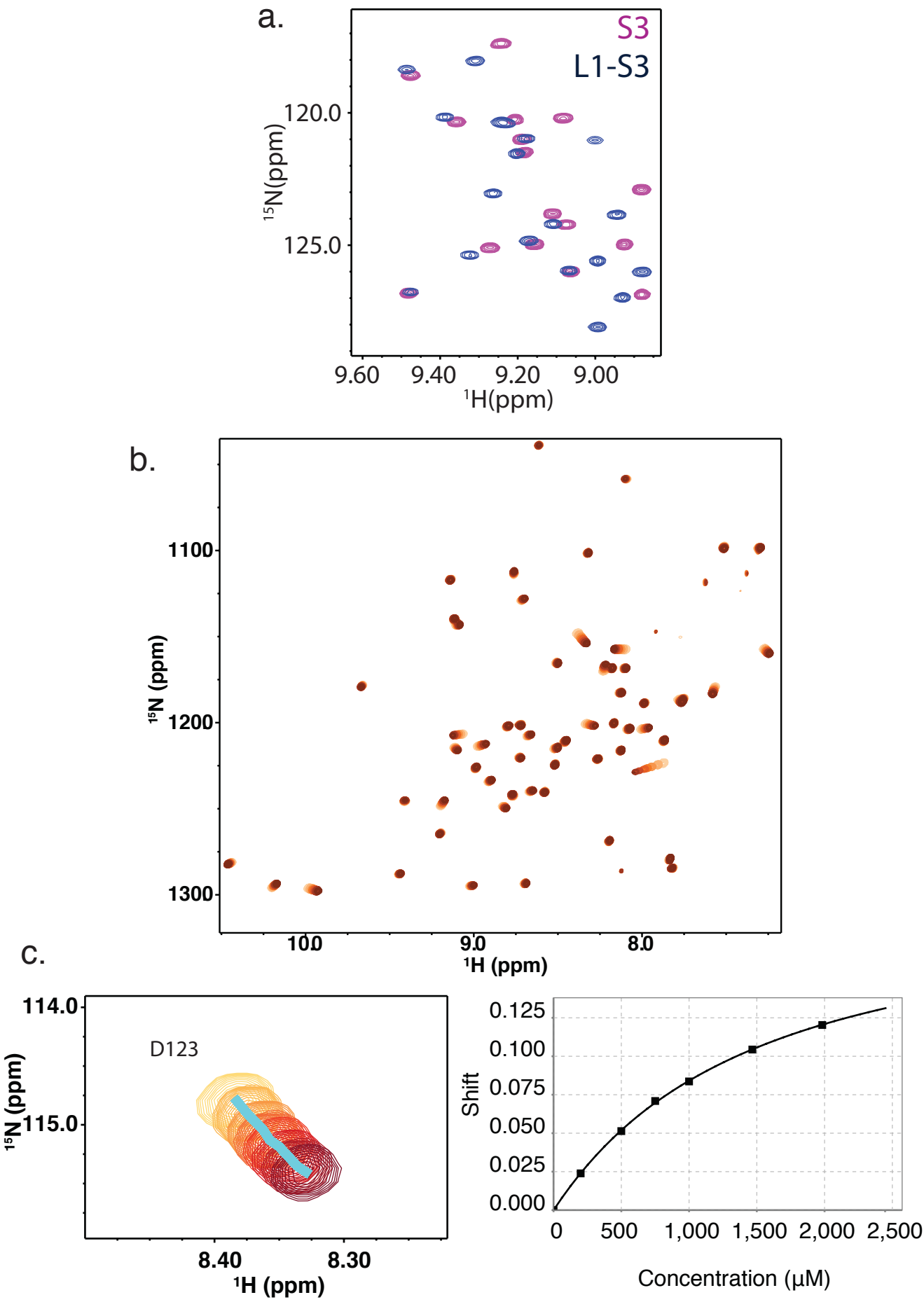
a.
S3
L1-S3
120.0
125.0
15N(ppm)
9.60
9.40
9.20
9.00
1H(ppm)
b.
1100
1200
1300
15N (ppm)
10.0
9.0
8.0
1H (ppm)
c.
114.0
115.0
15N (ppm)
D123
8.40
8.30
1H (ppm)
0.125
0.100
0.075
0.050
0.025
0.000
Shift
0
500
1,000
1,500
2,000
2,500
Concentration (μM)

# Figure S8

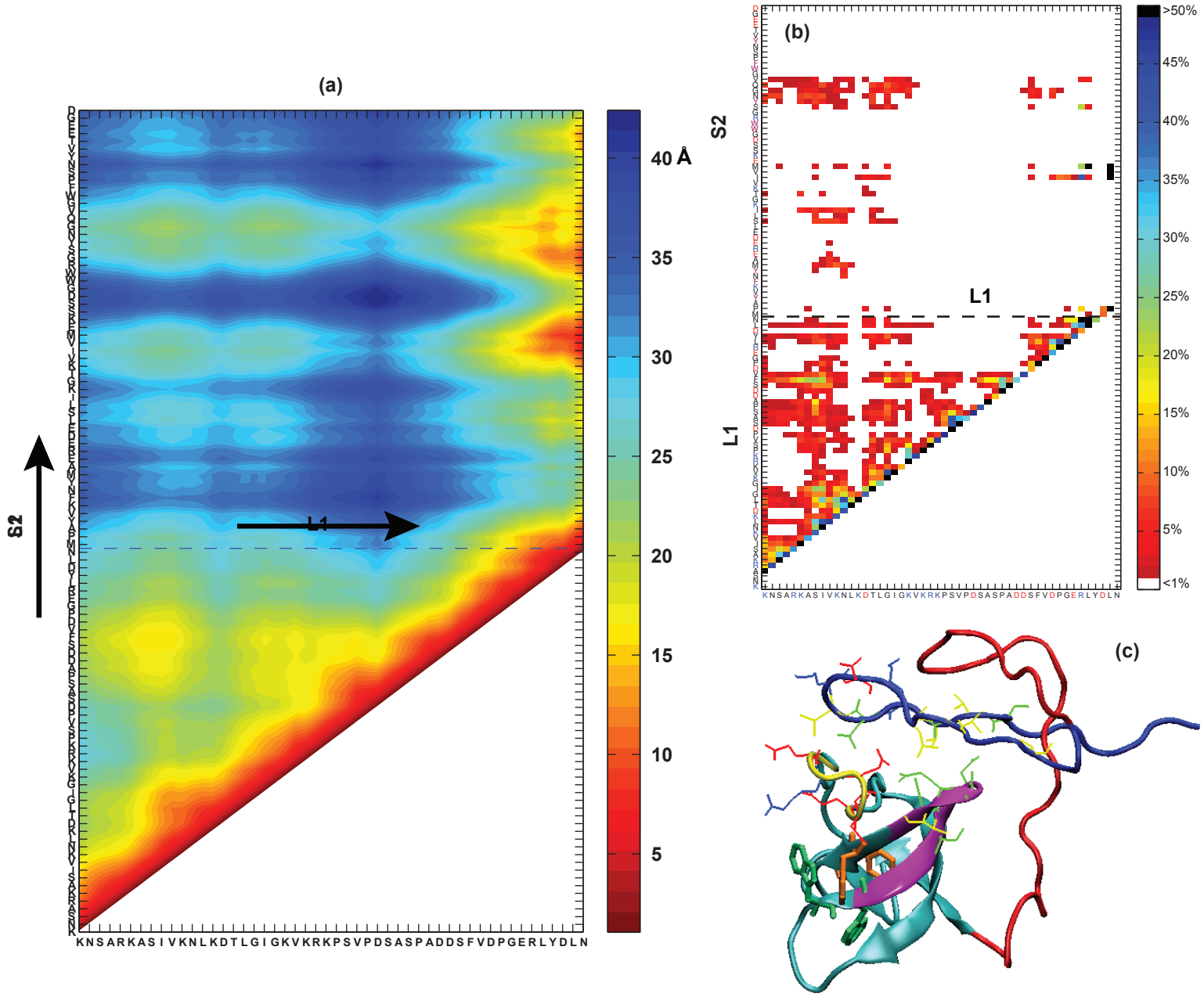
(a)
S2
L1
KNSARKASIVKNLKDTLGIGKVKRKPSVPDSASPADDSFVDPGERLYDLN
40 Å
35
30
25
20
15
10
5
(b)
S2
L1
L1
KNSARKASIVKNLKDTLGIGKVKRKPSVPDSASPADDSFVDPGERLYDLN
>50%
45%
40%
35%
30%
25%
20%
15%
10%
5%
<1%
(c)

Figure S9

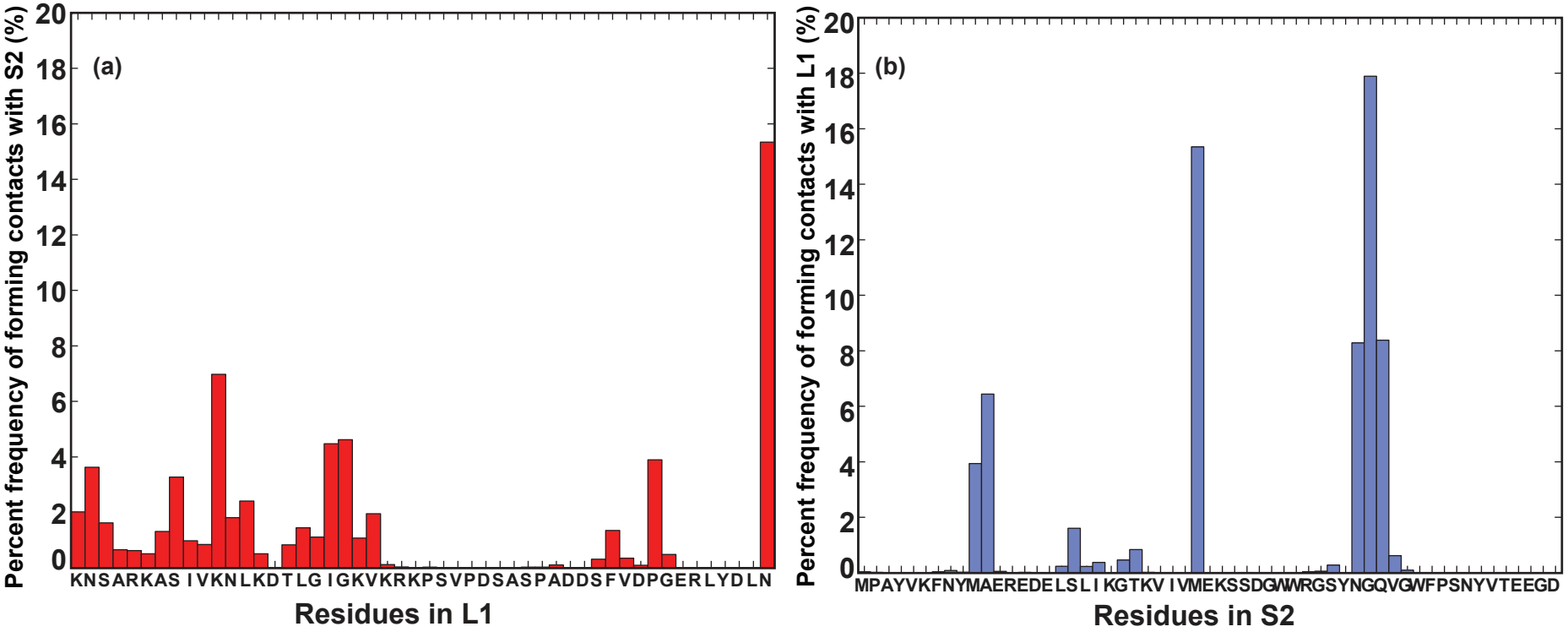
(a)
Percent frequency of forming contacts with S2 (%)
0
2
4
6
8
10
12
14
16
18
20
KNSARKAS I VKN LKD T LG I GKVKRKPSVPDSASPADDSFVDPGERLYDLN
Residues in L1
(b)
Percent frequency of forming contacts with L1 (%)
0
2
4
6
8
10
12
14
16
18
20
MPAYVKFNYMAEREDELSLI KGTKV I VMEKSSDGWWRGSYNGQVGWFPSNYVTEEGD
Residues in S2

# Figure S10